DOI:
10.1002/pmic.v10:3

Document Version
Peer reviewed version

Published in final edited form as:
Proteomics. 2010 February ; 10(3): 496–505. doi:10.1002/pmic.200900346.

Mesoporous Silica Chips for Selective Enrichment and Stabilization of Low Molecular Weight Proteome

Ali Bouamrani[‡,1], **Ye Hu**[‡,2], **Ennio Tasciotti**[‡,1], **Li Li**[3], **Ciro Chiappini**[2], **Xuewu Liu**[†,1], and **Mauro Ferrari**[*,†,1,2,4,5]

[1]Department of Nanomedicine and BioMedical Engineering, University of Texas Health Science Center at Houston, Houston TX 77030

[2]Department of Biomedical Engineering, University of Texas at Austin, Austin TX 78712

[3]Research Center of Protein Chemistry and Proteomic Core Laboratory, Brown Institute of Molecular Medicine, University of Texas Health Science Center at Houston, Houston TX 77030

[4]Department of Experimental Therapeutics, University of Texas MD Anderson Cancer Center, Houston TX 77030

[5]Department of Bioengineering, Rice University, Houston TX 77030

Abstract

The advanced properties of mesoporous silica have been demonstrated in applications which include chemical sensing, filtration, catalysis, drug-delivery and selective biomolecular uptake. These properties depend on the architectural, physical and chemical properties of the material, which in turn are determined by the processing parameters in evaporation-induced self-assembly. In this study, we introduce a combinatorial approach for the removal of the high molecular weight proteins and for the specific isolation and enrichment of low molecular weight species. This approach is based on Mesoporous Silica Chips able to fractionate, selectively harvest and protect from enzymatic degradation, peptides and proteins present in complex human biological fluids. We present the characterization of the harvesting properties of a wide range of mesoporous chips using a library of peptides and proteins standard and their selectivity on the recovery of serum peptidome. Using matrix-assisted laser desorption/ionization time-of-flight mass spectrometry, we established the correlation between the harvesting specificity and the physico-chemical properties of mesoporous silica surfaces. The introduction of this mesoporous material with fine controlled properties will provide a powerful platform for proteomics application offering a rapid and efficient methodology for low molecular weight biomarker discovery.

Keywords

Nanotechnology; Prefractionation techniques; Mass spectrometry; Surface modification; Peptide stabilization

*Corresponding author information: Mauro Ferrari, Ph.D., Division of Nanomedicine, Department of Biomedical Engineering, University of Texas Health Science Center, 1825 Pressler St. Suite 537, Houston, TX, 77030, mauro.ferrari@uth.tmc.edu, Tel (713)-500-2444, Fax (713)-500-2462 .
‡Shared first authorship.
†Shared senior authorship.

Competing financial interests
The authors declare no competing financial interests.

1 Introduction

The introduction of proteomic tools, especially development in mass spectrometry (MS)[1,2], has allowed the investigation of complex proteomes and the identification of proteins in cells, tissues and body fluids, increasing the interest of proteomic biomarker research[3,4]. Many studies suggest that the circulating peptidome is correlated to the pathological status of the patient [4-6]. A critical aspect of the development of MS based proteo- and peptido-mics is the broad assortment of molecular species in blood, with concentrations ranging over more than 10 orders of magnitude [7]. This wide dynamic range limits the detection of disease-related peptides present in trace amounts within a large background of abundant and non-relevant proteins. Despite the advances in protein analysis [8,9], the detection of low abundant markers and Low Molecular Weight (LMW) species remains a critical challenge [10-12]. Current strategies to resolve complex proteomes require sample fractionation and depletion prior to MS analysis, limiting throughput and introducing other concerns for experimental variability, reproducibility, sample handling procedures and protein stability during sample processing [13-16]. Innovative technologies addressing these issues are mandatory for biomarkers discovery. The development of nanomaterials, with controllable features offering advantageous new physico-chemical properties, has widely improved the use of nanotechnology in biomedical applications. The discovery of mesostructured materials in 1990s [17,18] boosted a great deal of research on the preparation [19-23], characterization [24] and morphological control [25,26] of surfactant-templated mesoporous materials. In previous work, we demonstrated the proof-of principle of LMW molecular uptake in mesoporous particles [27] and surfaces [28,29]. With tunable pore dimension, pore texture, and surface properties, the mesoporous films are the perfect tools for proteomics applications. In this study, we engineered Mesoporous Silica Chips (MSC) with organized pore structures and a wide range of pore sizes and showed the correlation between the surface properties at the nanoscale and the selectivity in the recovery of proteins and peptides. We further demonstrated the conservation and the long-term stability of proteins and peptides in the porous matrix of the MSC and evaluated the efficiency and reproducibility of this technology for the investigation of complex biological samples.

2 Materials and methods

2.1 Fabrication of mesoporous proteomic chips

The coating solution was prepared by starting with the hydrolyzed silicate precursor solution. Firstly, we added 14 ml of tetraethylorthosilicate (TEOS) into the mixture of 17 ml of ethanol, 6.5 ml of deionized water and 2 ml of 2M HCl under strong stirring. The silica sol-gels were ready for use after being heated at 75°C for 2 hours. The polymer template solutions were prepared by the addition of tri-block copolymer (BASF: L31, L35, L64, L121, P123, F38, F88, F108, F127) in 10 ml of ethanol at room temperature. For the preparation of mesoporous silica films with large pore size, a swelling agent, Polypropyleneglycol (PPG) or 1, 3, 5-Trimethyl benzene (TMB) was added in the ethanol solution of polymer before mixing with silicate. The film was obtained by spin-coating the solution on a silicon wafer: 1.5 ml of coating solution was dispensed on a 4″ silicon wafer, and spun at 600rpm for 5 s followed by 3000rpm for 30 s. The coated film was aged in an oven at 80°C for 15 h. The oven temperature was raised to 425°C at a rate of 5°C /min. The wafer was kept at 425°C for 4 h, and slowly cooled to room temperature. Oxygen plasma treatment was performed in a Plasma Asher (March Plasma System). Coating of Hexamethyldisilazane (HMDS) was performed in a HMDS vapor prime oven (YES) at 150°C for 5 min.

2.2 Characterization

The thickness and porosity of the obtained films were measured with a variable angle spectroscopic ellipsometer (J. A. Woollam Co. M-2000DI). Ellipsometric values, Δ and ψ were measured in the 300-1000nm range at three incidence angles, 55°, 60°, 65°, respectively, and fitted using the Effective Medium Approximation (EMA) model with WVASE32 software. The surface area and pore size of the mesoporous films were measured using N_2 adsorption-desorption isotherms on a Quantachrome Autosorb-3B Surface Analyzer. Nanopore size distributions were calculated from the adsorption branch of the isotherms using Barrett-Joiner-Halenda (BJH) model. Contact angles of film surface were measured by a goniometer with captive bubble contact angle measurement.

2.3 Fractionation Procedure

We have selected twenty-six peptides and proteins with broad range of molecular weight (900-66,500 Da), isoelectric point (pI 4.0-10.2), and structure. Identity and purity of each peptide and protein was verified by MS and combined, dried by vacuum centrifugation, and stored at −20°C. The molecular weight standards solution was prepared in 135 μL of sterile, deionized water (the final concentration of each standard is presented in the Supporting Information Table 1). 10 μl of samples (standards solution or human serum) was spotted onto the mesoporous surface of the MSC. The samples were incubated for 30 minutes in a wet chamber (100% humidity) to prevent sample evaporation. MSC surface was washed 5 times with 15μL of sterile, deionized water. Proteins were eluted from the pores by using 10μl of a 1:1 mixture of acetonitrile and 0.1 % trifluoroacetic acid (TFA) (v/v).

2.4 Mass spectrometry

A matrix solution of 5 mg/ml α-cyano-4-hydroxycinnamic acid (αCHCA, Sigma) in a 1:1 mixture of acetonitrile and 0.1% TFA(v/v) and a saturated matrix solution of trans-3,5-dimethoxy-4-hydroxycinnamic acid (SA, Sigma) in 2:1 mixture of acetonitrile and 0.1 % TFA was used for LMW and HMW peptides and proteins respectively. Each sample was mixed with the appropriate matrix in a 1:3 ratio, and spotted in duplicate onto the MALDI plate. Mass spectra were acquired on a Voyager-DE™-STR MALDI-TOF (Applied Biosystems, Framingham, MA) mass spectrometer in liner positive-ion mode, using a 337nm nitrogen laser. Samples were evaluated at two m/z ranges. For the m/z range of 800-10,000 Da, setting were optimized at acceleration voltage 20 KV, grid voltage 19KV,guide wire voltage 1KV, delay time 180 ns, and low-mass gate 800. For the m/z range of 3,000-100,000 Da the instrument was optimized at acceleration voltage 25 KV, grid voltage of 23.25 KV, guide wire voltage 6.25KV, delay time of 500 ns and low mass gate 3,000. Each spectrum was the average of 300 laser shots. The spectra were calibrated externally using the ProteoMass standards of peptides and proteins (Sigma) in each mass range.

2.5 Data processing and statistics

The raw spectra were processed with the Voyager Data Explorer software version 4.0 (Applied Biosystems) and the data were exported to SpecAlign [30,31] software for pretreatment. All spectra were aligned using the PAFFT correlation method and intensity was normalized to total ion current (TIC). The baseline was corrected and the negative values were removed prior to analysis. Hierarchical clustering was performed using Cluster software and visualized with Treeview software. The MALDI Data (M/z peak intensities) were log-transformed, normalized and median centered. Pearson correlation was used to calculate the distance between the samples, and complete linkage clustering was performed [32]. For supervised hierarchical clustering, an independent Student t-test was used for comparison between groups (n = 2 groups) for each detected MS peak. A P value of 0.02 or lower was considered significant to select differentially harvested peptides and proteins among the different mesoporous proteomic

chips (Large pores vs. Small pores, Hydrophobic vs. Hydrophilic, the swelling agents TMB vs. PPG).

3 Results and discussion

3.1 Fabrication and characterization of mesoporous proteomic chips

The MSC were produced by the evaporation induced self-assembly (EISA) procedure under acidic conditions using Pluronic triblock copolymers as structural templates [33,34]. The pH of precursor solutions was controlled at 1.5 to prevent the precipitation of mesoporous silicate and balance the procedure between the silicate hydrolysis and condensation of hydrolyzed silicate to polymer micelle. In Fig. 1 are illustrated the schematics of the chemical composition of the coating solution during the production of the mesoporous silica films and the assembly of the final chips (Fig. 1a-d). Manufacturing protocols were optimized to obtain smooth, crack-free surfaces across 4″ silicon wafers as verified by SEM and TEM imaging of the chip's cross sections (Fig. 1e-f). Porosity was related to the ratio between copolymer and TEOS, while the thickness was determined by many factors, including the concentration of surfactant, the spin-coating speed, and the aging time of the coating solution. The pore alignment was induced by strain during the spin-coating process [35]. The N_2 adsorption-desorption isotherms of six selected MSC are shown in Fig. 2a. The isotherms can be classified as Type-IV curve with H2 hysteresis loops, according to the standard of the International Union of Pure and Applied Chemistry [36]. This type of hysteresis indicated ink-bottle shaped pores, and non-ordered worm-like pore arrangement. For this type of isotherm, adsorption branch of the isotherm can be used to calculate the pore size distribution. The pore size distribution curves (values ranging from 2.7 nm to 9 nm) were derived from adsorption isotherms using Barrett-Joyner-Halenda (BJH) method (Fig. 2a right panel).

The reflection Small Angle X-ray Scattering (SAXS) curves of the films are shown in Fig. 2b. The curves were recorded 2cm off the center of the 4″ wafer, with the beam incidence along the direction of radius. The SAXS curve showed a peak around 0.5°-0.7° (corresponding to d-space around 13-17 nm) suggesting a periodic order in the spatial variation of the electron density in the film, and some degree of alignment of the pores. This was further confirmed by AFM measurement of the film surface (Fig. 2c). The image showed different dimensions of the features along and perpendicular to the radius.

Different chemical modifications were also studied. Oxygen plasma treatment was applied to ensure the hydrophilicity, while HMDS coating was applied to make the surface hydrophobic. The hydrophilicity of the films was evaluated through contact angle measurement. The O_2 plasma treated films showed <15° contact angle, while the HMDS coated film showed >65° contact angle (see Supporting Information Table 2 and Fig 1 for detailed properties of the different mesoporous surfaces and TEM images).

3.2 Enrichment of the LMW proteome

High-throughput mass spectrometry is a gold standard for protein expression profiling and for disease-related biomarker discovery [1]. However, the current MS technologies are not able to profile the entire proteome and particularly the LMW species because of the interfering signals generated by the highly abundant, High Molecular Weight (HMW) proteins [9]. To address this limitation, we developed a fractionation method using the MSC to efficiently and specifically enrich the LMW proteome from complex biological samples. The principle of this fast on-chip fractionation strategy is shown in Fig. 3a: 1- The sample is spotted on the chip surface and LMW molecules are trapped into the pores during the incubation step; 2- The larger protein species remain outside the pores and are removed during the washing steps; 3- The enriched small molecules are then eluted from the pores and further analyzed by MS. In order

to evaluate the fractionation and enrichment efficacy of this on-chip strategy, and to characterize how the physico-chemical properties of the chips correlate with their harvesting properties, we have selected 26 standard peptides and proteins with a broad range of molecular weights (900-66,500 Da) and isoelectric points (pI 4.0-10.2), and we have combined them to represent the diversity and complexity of biological samples (See Supporting information Fig. 2 and Table 1). Fig. 3b and 3c show the high detection signals of the standards when separated into two different solutions for the peptide range (16 markers from 900 to 8500 Da) and the protein range (16 markers from 3400 to 66500 Da). When combined in a unique solution, the detection signal in the peptide range dramatically decreased while the larger proteins remained well detected (Figure 3d and 3e). The MS detection signal suppression in the LMW observed with the combined solution of molecular markers mimics the results obtained with MS analysis of complex body fluids such as serum and plasma. The presence of higher amount of HMW molecules such as Albumin and other large proteins impede the detection of the LMW species. The results presented in Figures 3f and 3g demonstrate the ability to eliminate the big proteins and to increase significantly the detection of the LMW peptides and proteins.

The capacity of mass spectrometry approaches to investigate low abundant proteins in biological samples composed of highly complex proteomes such as serum body fluids is a major issue for the detection of potential biomarkers [2,3,10]. To assess the limit of detection of our technology, human serum sample was spiked with a known peptide (Neurotensin, 1673 Da) at different concentration levels before MSC fractionation and MALDI analysis. The results presented in Fig. 4 demonstrated the ability of the method to identify the spiked neurotensin in a concentration as low as 2ng/mL.

3.3 Pore size selectivity of the LMW enrichment

In order to assess the size-dependant depletion of HMW proteins, we have developed 6 proteomic chips with pore sizes ranged from 2.0 nm to 11.7 nm. A variety of pore sizes was first obtained by using different polymer templates with different volume ratio of hydrophilic/hydrophobic composition. Because of its highest hydrophobic/hydrophilic ratio among pluronic surfactants, L121 is capable of forming the mesoporous silica with the largest porosity (~55%) and pore size (5.2 nm). In addition, by applying a different ratio of swelling agent such as Poly Propylene Glycol (PPG) to the L121 pluronic surfactant, the pore size has been further enlarged to obtain MSC with 7.4 nm, 9.0 nm and 11.7 nm. To evaluate the molecular cut-off and the enrichment properties of the different pore sizes, we fractionated the solution of peptide and protein standards on the set of MSC ranging from 2.0 to 11.7 nm. The removal of the large proteins is size dependant as illustrated by the gradual decrease of the molecular cut-off observed for the different chips (Fig. 5a). The silica surface with 9.0 nm pores did not completely exlude albumin, accordingly to its three-dimensional structure which exhibits an average size of 8 by 3 nm[37]. This analysis demonstrates the size exclusion principle of the mesoporous chip fractionation, and reveals the limit of this depletion approach observed with the 11.7 nm pores which provides a similar MS pattern to the non-fractionated sample (Fig. 5b). In addition to the size-dependant depletion of HMW proteins, the on-chip fractionation of the standards solution displays a differential and selective enrichment of LMW species associated with the pore sizes. The two-way hierarchical clustering presented in Fig. 5c shows the LMW standards enrichment pattern obtained with the different MSC. Even if all the peptides are below the molecular cut-off of the chips, there is a positive correlation between the pore sizes and the molecular weight of the trapped species. The MSC with large pores, up to 9 nm, preferentially harvest bigger peptides, while smaller peptides are recovered more efficiently by the chips with smaller pores. The chips with 11.7 nm pores present no significant improvement in the LMW region detection (Fig. 5d). This result indicates the size limit of the MSC for an efficient enrichment strategy.

3.4 Identification of the selective fractionation patterns due to MSC's nanofeatures

In the analysis of the fractionation and enrichment of LMW species from human serum, we subdivided the chips in 3 categories according to: 1) pore size; 2) wettability; 3) pore geometry and surface morphology. We performed unsupervised two-way hierarchical clustering (two-dimensional complete linkage) to analyze the overall MALDI profiles of the different MSC. (Fig. 6a). Depending on their harvesting characteristics, selective nanopore size and specific recovery patterns, each of the MSC consistently identified unique proteomic signatures, as shown in the supervised hierarchical clustering (Fig. 6b-d). Using a multi-chip strategy and combining the MS profiles obtained from five different MSC we obtained a three fold increase in the number of detected peptides and proteins in the LMW range with respect to plain unprocessed serum (Fig. 6e-f and Supporting Information Fig. 5). These results showed that the different nanofeatures (structure, size and chemistry of the pores) on the MSC conveyed different functionalities and served as analytical "first order processors" of this technology. According to this strategy, a multitude of chips can be used simultaneously to increase the amount of information recovered from the serum.

3.5 Sample stability and reproducibility of the harvesting procedure

Reproducibility and reliability are crucial factors for any assay to be used in the clinical setting. Several publications reported that pre-analytical sample management might lead to significant alterations of the proteomic profiles and the generation of artifacts [13,16]. We assessed the consistency of our on-chip fractionation assay reproducing the same experiment in 6 replicates. After fractionation, the spectra of the replicates showed highly reproducible MS signals (Supporting information Fig. 6). To evaluate protein stability, the MSC were incubated with human serum, dried after washing, and stored for 3 weeks at room temperature. The protein/peptide patterns obtained were comparable with those of freshly fractionated serum (Fig. 7a), as confirmed by the results of the statistical analysis showed in Fig. 7c. The variability of the peak signals measured by the average Coefficient of Variation (CV) was estimated at 12.7 % for crude serum and at 14.2% for the fractionated samples. The marginal variations could be due to the internal variability of the MALDI instrument and suggested that the on-chip pretreatment and storage did not induce any significant alteration of the MS protein profiles. The same experiment has been performed on non porous silicon. The dried serum recovered after storage on silicon surface was fractionated on the MSC before MALDI analysis. The poor MS profile obtained demonstrated the stabilization advantage of the mesoporous surface. In analogy with previously postulated mechanisms, we hypothesize that the LMW species trapped inside the nanopores were preserved from degradation through the size exclusion of proteases, or by steric inhibition of their proteolytic activity in the confined space of the nanopores [38, 39].

The establishment of a simple sample acquisition and storage protocol, and the ability to impede further degradation of the proteins and peptides once they are captured, are essential for translation into the laboratory clinical practice [40,41]. With prior methodologies, deceptive results confounded the analysis and rendered meaningless the use of the profiles to derive any significant diagnostic or clinical information [10,11,41]. On the contrary, after processing on the MSC, the resulting protein patterns were reproducible and consistent even after long term on-chip storage at room temperature.

4 Concluding remarks

Using surfactant-templated mesoporous silica thin films, we have developed a size-exclusion method for a rapid and specific isolation and analysis of LMW peptides from complex biological samples. In combination with mass spectrometry profiling, we have demonstrated significant improvement and optimization of the specific harvesting efficacy of the MSC.

Besides the HMW proteins depletion, we established the correlation between the harvesting capacity and the physico-chemical properties of mesoporous silica surfaces. The structural design and the chemical functionalization of the porous silica surface further increase the specificity of peptides enrichment. The wealth of finely tunable and controlled properties on mesoporous silica surfaces could be used for MS-based peptide and protein profiling of complex biological fluids providing a powerful tool in the selective separation and concentration of the low molecular weight proteome.

The MSC are inexpensive to manufacture, and allow for scaled up production to attain the simultaneous processing of a large number of samples, providing advantageous features for exploratory screening and biomarker discovery. They may further be used to store, protect and stabilize biological fluids, enabling the simplified and cost-effective collection and transportation of clinical samples.

Supplementary Material

Refer to Web version on PubMed Central for supplementary material.

Acknowledgments

The authors thank Prof. Rowen Chang and the Research Center of Protein Chemistry Core Laboratory at the university of Texas health science center at Houston for the use of the Mass Spectrometry facility, M. Landry for excellent graphical support, and Y. Flores, Jimenez, M. Way and K. Dara for laboratory assistance. We thank the Microelectronics Research Center, the Texas Materials Institute and the Center for Nanomaterials, at the University of Texas at Austin, for the use of materials fabrication and characterization facilities. We thank Dr. Elizabeth Donnachie, Research Associate in the Gulf States Hemophilia and Thrombophilia Center at UTHSC-Houston, for providing the serum used in the study.

These studies were supported by the following grants: State of Texas's Emerging Technology Fund, NIH (R21/R33CA122864), NASA (NNJ06HE06A), NIH (R01CA128797), DoD CDMRP Breast Cancer Research Program Innovator Award (W81XWH-08-BCRP-INNOV). The authors would like to recognize the contributions and support from the Alliance for NanoHealth (ANH).

References

[1]. Aebersold R, Mann M. Mass spectrometry-based proteomics. Nature 2003;422:198–207. [PubMed: 12634793]

[2]. Hanash SM, Pitteri SJ, Faca VM. Mining the plasma proteome for cancer biomarkers. Nature 2008;452:571–579. [PubMed: 18385731]

[3]. Kulasingam V, Diamandis EP. Strategies for discovering novel cancer biomarkers through utilization of emerging technologies. Nat Clin Pract Oncol 2008;5:588–599. [PubMed: 18695711]

[4]. Liotta LA, Ferrari M, Petricoin E. Clinical proteomics: written in blood. Nature 2003;425:905. [PubMed: 14586448]

[5]. Villanueva J, Shaffer DR, Philip J, Chaparro CA, et al. Differential exoprotease activities confer tumor-specific serum peptidome patterns. J Clin Invest 2006;116:271–284. [PubMed: 16395409]

[6]. Petricoin EF, Belluco C, Araujo RP, Liotta LA. The blood peptidome: a higher dimension of information content for cancer biomarker discovery. Nat Rev Cancer 2006;6:961–967. [PubMed: 17093504]

[7]. Anderson NL, Anderson NG. The human plasma proteome: history, character, and diagnostic prospects. Mol Cell Proteomics 2002;1:845–867. [PubMed: 12488461]

[8]. Shores KS, Knapp DR. Assessment approach for evaluating high abundance protein depletion methods for cerebrospinal fluid (CSF) proteomic analysis. J Proteome Res 2007;6:3739–3751. [PubMed: 17696521]

[9]. Tirumalai RS, Chan KC, Prieto DA, Issaq HJ, et al. Characterization of the low molecular weight human serum proteome. Mol Cell Proteomics 2003;2:1096–1103. [PubMed: 12917320]

[10]. Diamandis EP. Mass spectrometry as a diagnostic and a cancer biomarker discovery tool: opportunities and potential limitations. Mol Cell Proteomics 2004;3:367–378. [PubMed: 14990683]

[11]. Petricoin EF, Ardekani AM, Hitt BA, Levine PJ, et al. Use of proteomic patterns in serum to identify ovarian cancer. Lancet 2002;359:572–577. [PubMed: 11867112]

[12]. Villanueva J, Philip J, Chaparro CA, Li Y, et al. Correcting common errors in identifying cancer-specific serum peptide signatures. J Proteome Res 2005;4:1060–1072. [PubMed: 16083255]

[13]. Findeisen P, Sismanidis D, Riedl M, Costina V, Neumaier M. Preanalytical impact of sample handling on proteome profiling experiments with matrix-assisted laser desorption/ionization time-of-flight mass spectrometry. Clin Chem 2005;51:2409–2411. [PubMed: 16306114]

[14]. Georgiou HM, Rice GE, Baker MS. Proteomic analysis of human plasma: failure of centrifugal ultrafiltration to remove albumin and other high molecular weight proteins. Proteomics 2001;1:1503–1506. [PubMed: 11747208]

[15]. Rabilloud T. Two-dimensional gel electrophoresis in proteomics: old, old fashioned, but it still climbs up the mountains. Proteomics 2002;2:3–10. [PubMed: 11788986]

[16]. Seam N, Gonzales DA, Kern SJ, Hortin GL, et al. Quality control of serum albumin depletion for proteomic analysis. Clin Chem 2007;53:1915–1920. [PubMed: 17890439]

[17]. Beck JS, Vartuli JC, Roth WJ, Leonowicz ME, et al. A New Family of Mesoporous Molecular-Sieves Prepared with Liquid-Crystal Templates. Journal of the American Chemical Society 1992;114:10834–10843.

[18]. Kresge CT, Leonowicz ME, Roth WJ, Vartuli JC, Beck JS. Ordered Mesoporous Molecular-Sieves Synthesized by a Liquid-Crystal Template Mechanism. Nature 1992;359:710–712.

[19]. Attard GS, Glyde JC, Goltner CG. Liquid-Crystalline Phases as Templates for the Synthesis of Mesoporous Silica. Nature 1995;378:366–368.

[20]. Huo QS, Margolese DI, Ciesla U, Feng PY, et al. Generalized Synthesis of Periodic Surfactant Inorganic Composite-Materials. Nature 1994;368:317–321.

[21]. Miyata H, Kuroda K. Preferred alignment of mesochannels in a mesoporous silica film grown on a silicon (110) surface. Journal of the American Chemical Society 1999;121:7618–7624.

[22]. Yang P, Deng T, Zhao D, Feng P, et al. Hierarchically ordered oxides. Science 1998;282:2244–2246. [PubMed: 9856944]

[23]. Zhao DY, Feng JL, Huo QS, Melosh N, et al. Triblock copolymer syntheses of mesoporous silica with periodic 50 to 300 angstrom pores. Science 1998;279:548–552. [PubMed: 9438845]

[24]. Sakamoto Y, Kaneda M, Terasaki O, Zhao DY, et al. Direct imaging of the pores and cages of three-dimensional mesoporous materials. Nature 2000;408:449–453. [PubMed: 11100722]

[25]. Wang JF, Zhang JP, Asoo BY, Stucky GD. Structure-selective synthesis of mesostructured/mesoporous silica nanofibers. Journal of the American Chemical Society 2003;125:13966–13967. [PubMed: 14611226]

[26]. Yamaguchi A, Uejo F, Yoda T, Uchida T, et al. Self-assembly of a silica-surfactant nanocomposite in a porous alumina membrane. Nat Mater 2004;3:337–341. [PubMed: 15077106]

[27]. Terracciano R, Gaspari M, Testa F, Pasqua L, et al. Selective binding and enrichment for low-molecular weight biomarker molecules in human plasma after exposure to nanoporous silica particles. Proteomics 2006;6:3243–3250. [PubMed: 16645983]

[28]. Gaspari M, Cheng MMC, Terracciano R, Liu XW, et al. Nanoporous surfaces as harvesting agents for mass spectrometric analysis of peptides in human plasma. Journal of Proteome Research 2006;5:1261–1266. [PubMed: 16674117]

[29]. Geho D, Cheng MM, Killian K, Lowenthal M, et al. Fractionation of serum components using nanoporous substrates. Bioconjug Chem 2006;17:654–661. [PubMed: 16704202]

[30]. Wong JW, Cagney G, Cartwright HM. SpecAlign--processing and alignment of mass spectra datasets. Bioinformatics 2005;21:2088–2090. [PubMed: 15691857]

[31]. Wong JW, Durante C, Cartwright HM. Application of fast Fourier transform cross-correlation for the alignment of large chromatographic and spectral datasets. Anal Chem 2005;77:5655–5661. [PubMed: 16131078]

[32]. Eisen MB, Spellman PT, Brown PO, Botstein D. Cluster analysis and display of genome-wide expression patterns. Proc Natl Acad Sci U S A 1998;95:14863–14868. [PubMed: 9843981]

[33]. Lu Y, Ganguli R, Drewien CA, Anderson MT, et al. Continuous formation of supported cubic and hexagonal mesoporous films by sol-gel dip-coating. Nature 1997;389:364–368.

[34]. Yang H, Coombs N, Sokolov I, Ozin GA. Free-standing and oriented mesoporous silica films grown at the air-water interface. Nature 1996;381:589–592.

[35]. Rice RL, Kidd P, Holmes JD, Morris MA. Structural comparison of hexagonally ordered mesoporous thin films developed by dip- and spin-coating using X-ray reflectometry and other quantitative X-ray techniques. Journal of Materials Chemistry 2005;15:4032–4040.

[36]. Sing KSW, Everett DH, Haul RAW, Moscou L, et al. Reporting Physisorption Data for Gas Solid Systems with Special Reference to the Determination of Surface-Area and Porosity (Recommendations 1984). Pure and Applied Chemistry 1985;57:603–619.

[37]. He XM, Carter DC. Atomic structure and chemistry of human serum albumin. Nature 1992;358:209–215. [PubMed: 1630489]

[38]. Luchini A, Geho DH, Bishop B, Tran D, et al. Smart hydrogel particles: biomarker harvesting: one-step affinity purification, size exclusion, and protection against degradation. Nano Lett 2008;8:350–361. [PubMed: 18076201]

[39]. Vaitheeswaran S, Thirumalai D. Interactions between amino acid side chains in cylindrical hydrophobic nanopores with applications to peptide stability. Proceedings of the National Academy of Sciences 2008;105:17636–17641.

[40]. Banks RE, Stanley AJ, Cairns DA, Barrett JH, et al. Influences of blood sample processing on low-molecular-weight proteome identified by surface-enhanced laser desorption/ionization mass spectrometry. Clin Chem 2005;51:1637–1649. [PubMed: 16002455]

[41]. Ransohoff DF. Lessons from controversy: ovarian cancer screening and serum proteomics. J Natl Cancer Inst 2005;97:315–319. [PubMed: 15713968]

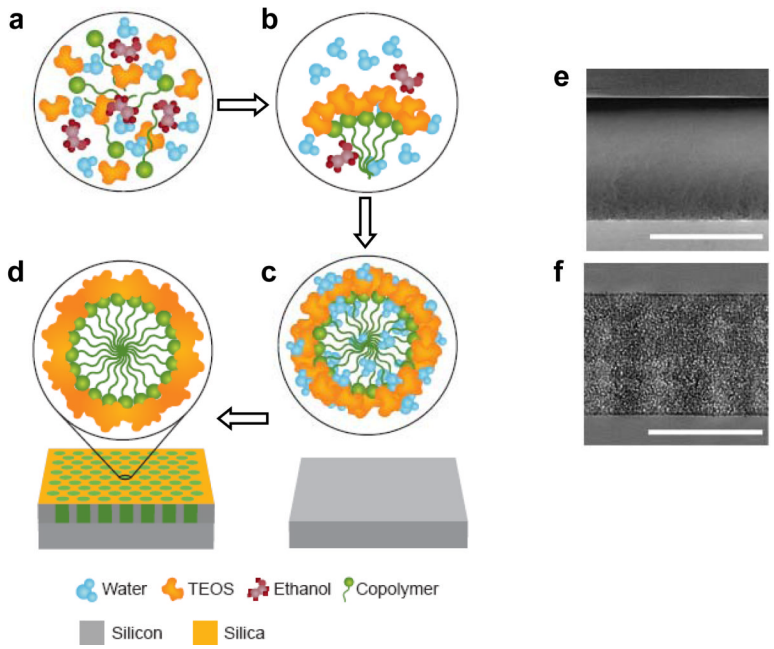

Figure 1. Production and assembly of MSC for proteomic applications

a-d, Schematic evolution of the chemical composition of the coating solution during the production of a mesoporous silica film. a, Fresh coating solution; b, Formation of micelles; c, Evaporation induced self assembly during spin-coating process; d, Zoomed in view of a pore after aging at elevated temperature. e, Bulk silicon wafer surface; f, Mesoporous silica film on a bulk silicon wafer.

e-f, Cross-section of GX6 chip by SEM and TEM imaging respectively (scale bar is 500nm).

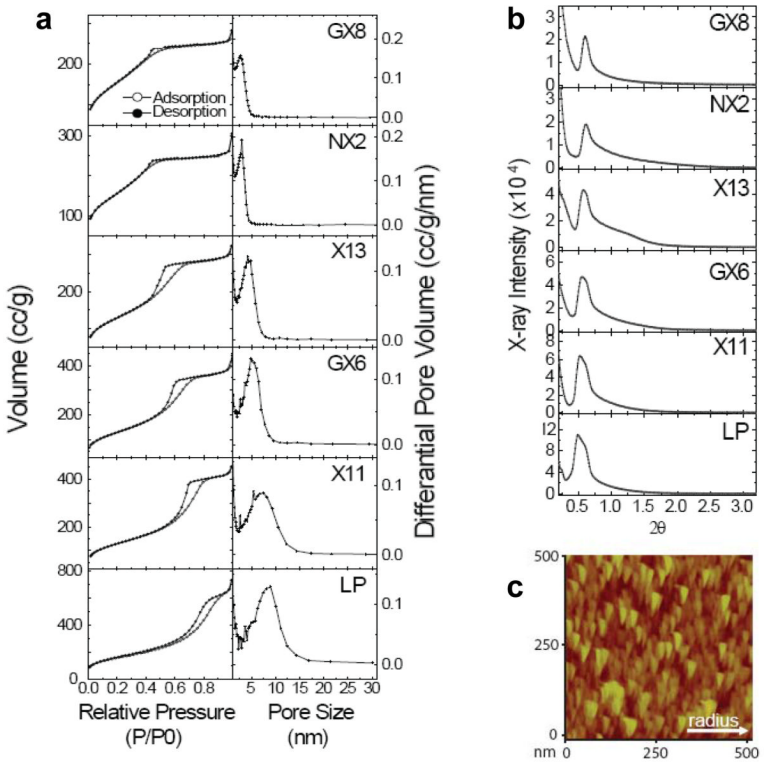

Figure 2. Physical characterization of the MSC

a, Left panel: N2 adsorption-desorption isotherms, Right panel: pore size distribution curve.

b, Reflection SAXS patterns for 8 selected MSC.

c, AFM image of the X11 chip.

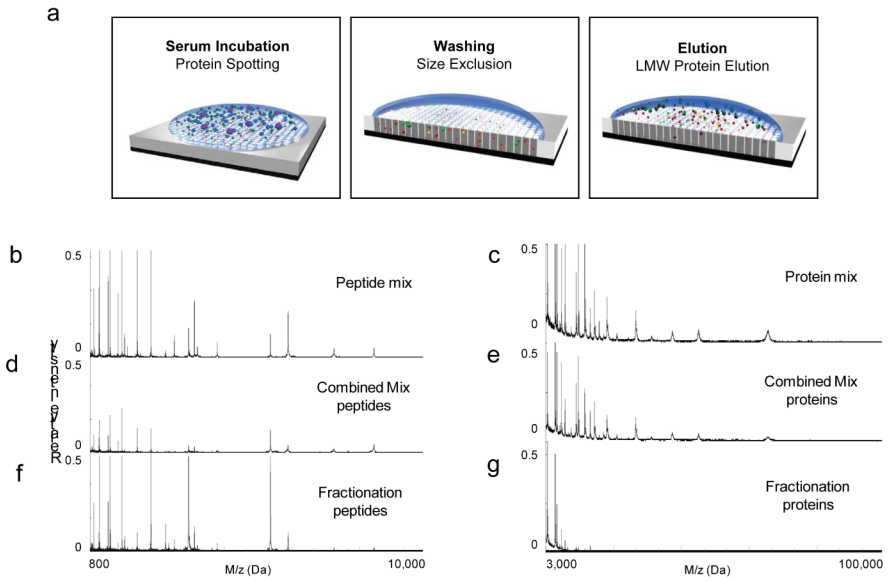

Figure 3. Principle of MSC fractionation and LMW enrichment

a, After sample spotting on the surface, LMW proteins and peptides are trapped into the pores while the larger species remained outside the pores and are removed during the washing steps. The enriched fractions are then eluted and analyzed by MALDI.

b-c, Detection of the molecular weight standards by MALDI-TOF in the peptide range (800 to 10000 Da) and in the protein range (3000 to 100000 Da). For the separated mixes of peptides (16 markers from 900 to 8500 Da) and proteins (16 markers from 3400 to 66500 Da), the profiles present a high level of detection for each species.

d-e, In the combined mix, the signal suppression of LMW standards is due to the high concentration of HMW proteins.

f-g, In the MALDI profiles of the combined standard mix after fractionation on the MSC, the detection of LMW markers is significantly increased compared to the unprocessed sample.

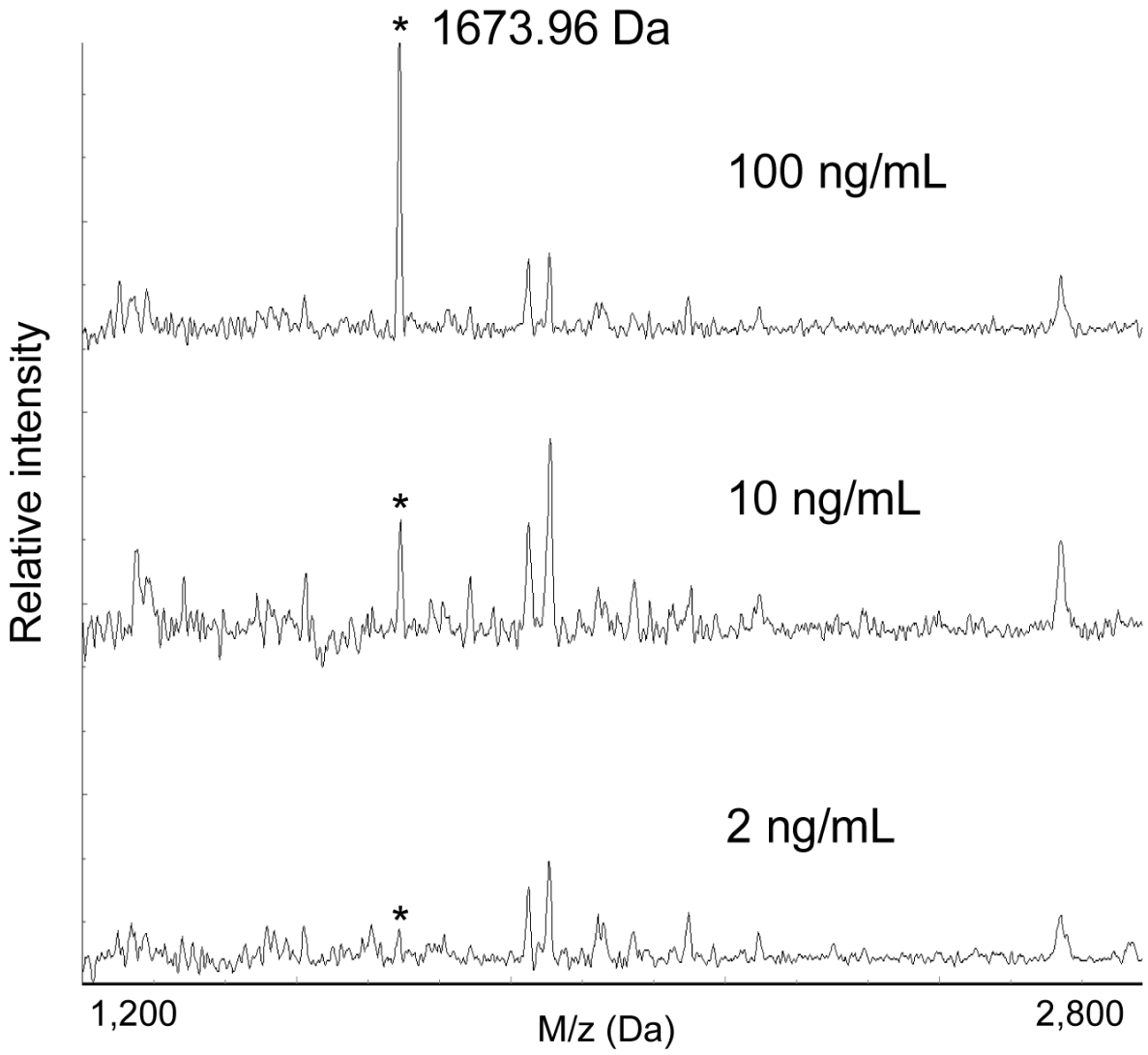

Figure 4. Sensitivity of the MSC enrichment

Mass spectra of spiked human serum sample with decreasing concentrations of neurotensin peptide (1673.96 Da): 100 ng/mL, 10 ng/mL and 2 ng/mL (from top to bottom).

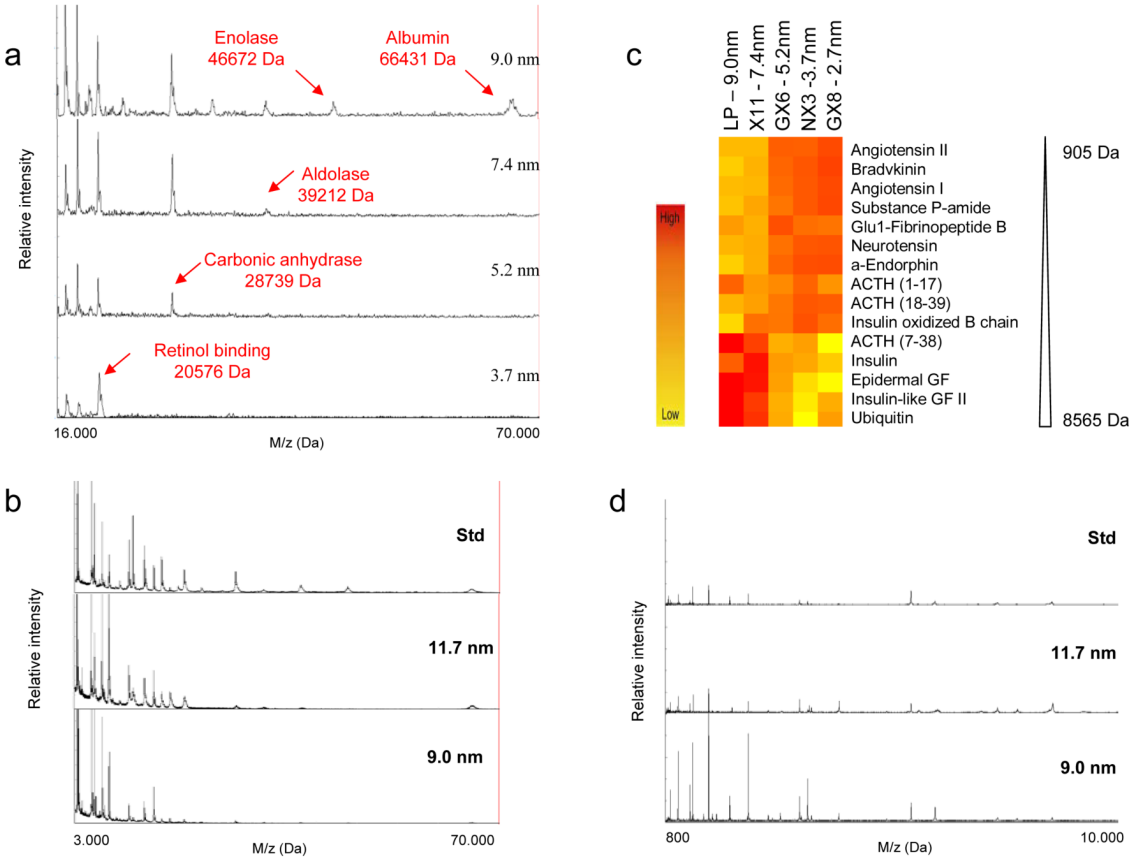

Figure 5. Molecular cut-off and size-dependent enrichment of the MSC

a, Magnified view of the MALDI spectra demonstrating the characteristic molecular cut-off of each MSC correlating to the pore size.

b, MALDI profiles of the HMW region for the standards solution before (Std) and after fractionation on 11.7 and 9.0 nm pores MSC.

c, Two-way hierarchical clustering of the peptide mix features among the different chips. The intensity of the red or yellow color indicates the relative peptide concentration. Larger pores enhanced the harvesting of bigger peptides (from 3600 to 8500 Da), while the small peptides (from 900 to 3500 Da) were preferentially recovered from the chips with smaller pores.

d, MALDI profiles of the LMW region for the standards solution before (Std) and after fractionation on 11.7 and 9.0 nm pores MSC.

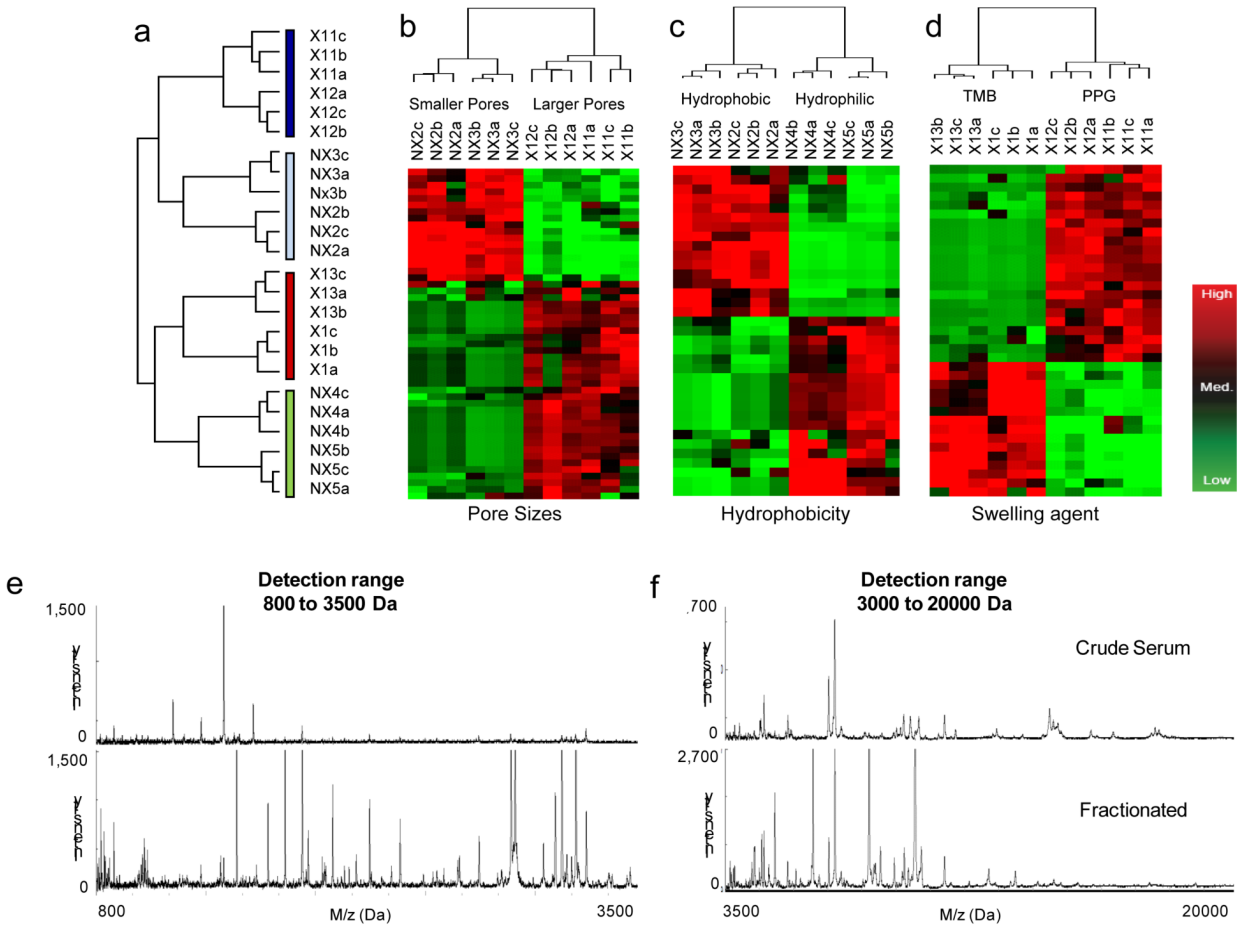

Figure 6. Effect of pore sizes and chemical properties on serum peptide harvesting

a, Dendogram of the unsupervised two-way hierarchical clustering. Each set of MSC is uniquely identified. The dark and light blue rectangles represent large and small pores, respectively. The green and red rectangles represent the hydrophobic-and TMB generated-MSC, respectively.

b-d, Supervised hierarchical clustering and specific recovery pattern for each set of MSC as indicated in the figure. The relative intensity is gradually indicated with red squares (high intensity), black squares (median) and green squares (low intensity or absence of a peak). The entire hierarchical clusters are presented in Supporting Information Fig. 3 and 4.

e-f, The MS profiles obtained from crude serum (e) or from purified peptides and proteins using the multi-chip strategy (f). The multi-chip profile was obtained by combining the spectrum from each MSC purified fraction.

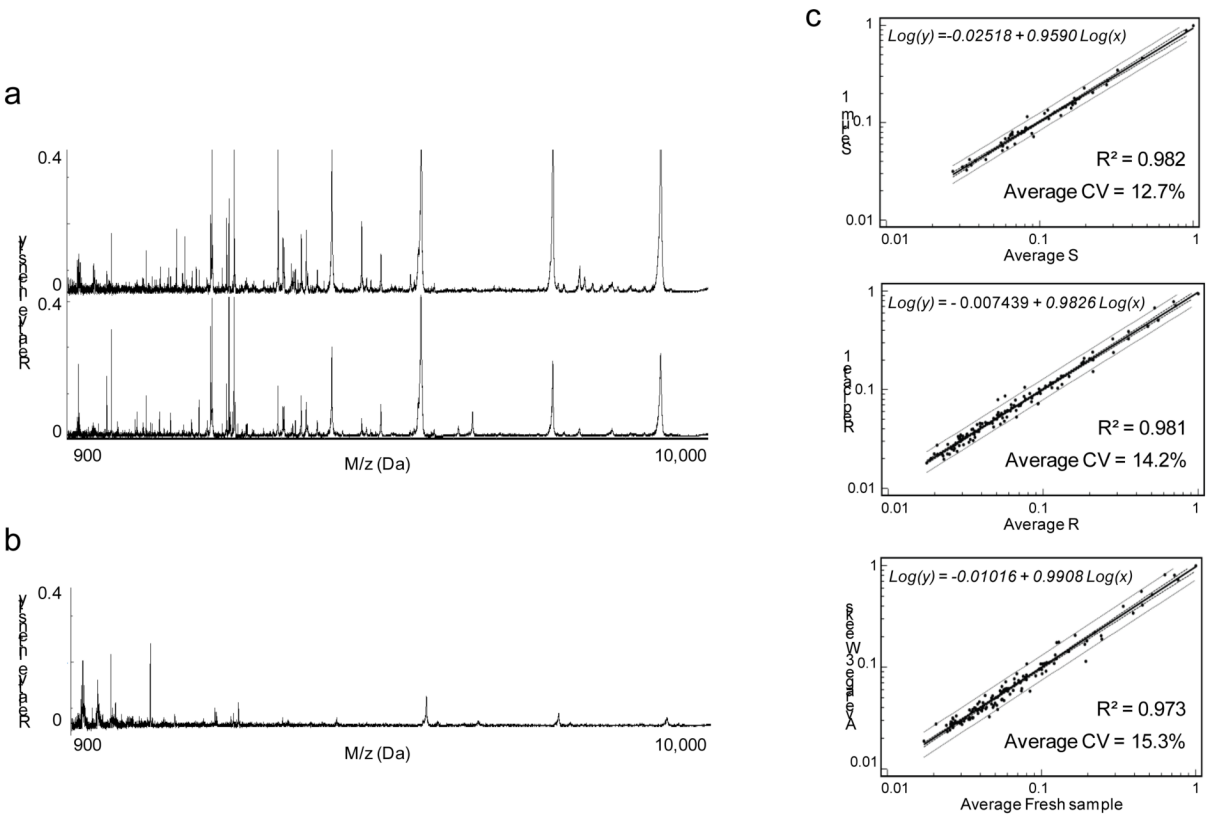

Figure 7. On-chip stabilization of fractionated serum

a, Representative MALDI profiles of LMW peptides and proteins eluted immediately after serum fractionation or after 3 weeks of on-chip storage at room temperature.

b, MS spectrum of LMW fraction of serum sample dried and stored on nonporous silicon surface.

c, From top to bottom: Linear regression analysis of average intensities of detected MS peaks in each replicate compared to replicate 1 for crude serum, freshly fractionated serum and fractionated serum after 3 weeks MSC storage at room temperature. Equation, coefficient of variation (CV) and coefficient of determination (R^2) are indicated.